

FORMATION OF MESOPOROUS GERMANIUM BY ELECTROCHEMICAL ETCHING FOR LIFT-OFF PROCESSES

E. Garralaga Rojas,^{1,*} B. Terheiden,¹ J. Hensen,¹ W. Köstler,² W. Zimmermann,² G. Strobl,² H. Plagwitz,¹ and R. Brendel¹

¹ Institut für Solarenergieforschung Hameln/Emmerthal (ISFH), Am Ohrberg 1, D-31860 Emmerthal, Germany

² AZUR SPACE Solar Power GmbH, Theresienstr. 2, D-74072 Heilbronn, Germany

*Tel: +49 5151 999 314, Fax: +49 5151 999 400, Email: e.garralaga@isfh.de

ABSTRACT: We present the formation of uniform thick mesoporous layers in Ge produced by means of electrochemical etching in highly concentrated HF electrolytes. The process is demonstrated on Ge wafers with 4 inch diameter, resulting in spatially homogenous porous layers. The formation of mesoporous Ge always takes place simultaneously with a constant dissolution of the already formed porous layer. The growth rate lies in the range of 0.071 to 2.7 nm/minute for etching current densities in a range of 0.1 to 80 mA/cm², while both etch and dissolution rates lie in the range of several $\mu\text{m}/\text{min}$. We define the substrate usage as the ratio of growth rate and etch rate. It is used to determine the porous layer growth efficiency and lies in the 0.2-2% range for anodic etching experiments. If the etching bias is alternated from anodic to cathodic periodically, substrate thinning is avoided and usage increases up to 98%.

Keywords: Germanium, Space, Layer transfer processes

1 INTRODUCTION

The reduction of weight of multi-junction III-V semiconductor solar cells is an important issue for space applications because of cost reduction on satellite system level due to reduced starting weight of the rocket. The current state-of-the-art III-V space solar cell is a monolithic Ga_{0.5}In_{0.5}P/Ga_{0.99}In_{0.01}As/Ge triple-junction cell grown lattice-matched on 100-150 μm substrates with begin-of-life (BOL) efficiencies in the 30 % range [1]-[3]. Multi-junction solar cells are usually formed by epitaxy on Ge substrate wafers. The substrate material determines the lattice constant of the stack, provides mechanical stability during the cell process, and serves as bottom cell. For reasons of mechanical stability, the substrate wafer is typically more than 100 μm thick, whereas a few μm thickness would be sufficient for its use as bottom cell. As a consequence, the heavy substrate wafers reduce the available payload for satellite missions. Separating the electrically active solar cells from their substrates by a lift-off process after the epitaxy, could solve this issue.

Several techniques allow weight reduction in the production of solar cells. The Ge or GaAs substrate wafers can be removed by etching [4] or grinding, which reduces weight but has the disadvantage that the substrate wafer is lost to further re-use. In contrast, the porous silicon (PSI) process uses a double layer of mesoporous Si formed by means of electrochemical etching for the production of monocrystalline thin-film Si solar cells [5]. A mesoporous layer with low porosity at the surface of the substrate is used as a seed layer for the Si epitaxy, while a buried highly porous layer is used as a pre-determined breaking-point. According to the IUPAC, the term mesoporous refers to pores with size in a range of 2 to 50 nm [6].

However, in order to apply such a process to III-V-based solar cells on Ge substrates, the formation of homogeneous electrochemically etched mesoporous Ge has to be shown. We recently demonstrated for the first time the formation of mesoporous Ge layers (PGe) by means of electrochemical etching [7]. In this work we review the key results that emerge from the formation of spatially homogeneous mesoporous Ge layers by means of anodic etching of 4 inch Ge wafers in HF-based electrolytes. The impact of the electrolyte concentration

and etching current densities on the morphology and thickness of the porous layers are investigated. The etching rates are determined for various etching durations and current densities. Thus this work lays the foundation of obtaining lightweight III-V-based solar cells, and to re-use the Ge substrate by applying a layer transfer process similar to the PSI process.

2 EXPERIMENTAL

Monocrystalline 4 inch p-type Ge wafers with specific resistivity values lying in a range between 10 and 35 m Ωcm are electrochemically etched in HF-based solutions. The polished wafers have a thickness of (150 ± 10) μm and their orientation is {100}. A double-container etching cell is used for anodizing the wafers. Aqueous hydrofluoric acid (HF) with a concentration varying in a range between 2 and 50 wt % serves as electrolyte. The potentiostat Elypor 3 from ET&TE Etch and Technology GmbH is computer-controlled and allows various current or voltage time-profiles in either galvanostatic or potentiostatic mode. Different profiles of current or voltage are studied. The etching time varies between 1 minute and 15 hours. Once the process is finished, the samples are rinsed in deionized water and dried under N₂ stream. The morphology and thicknesses of the porous layers are inspected in a high resolution Hitachi S-4800 Scanning Electron Microscope (SEM).

3 ANODIC ETCHING OF MESOPOROUS GERMANIUM

Figure 1 shows the cross-sectional SEM image of a sample after being etched and subsequently rinsed and dried. Randomly and uniformly distributed mesopores are obtained at the surface of the sample by using HF with concentrations in the range between 30 and 50 wt %. A Ge mesoporous layer with a thickness of 600 nm with two well-defined etching fronts can be observed.

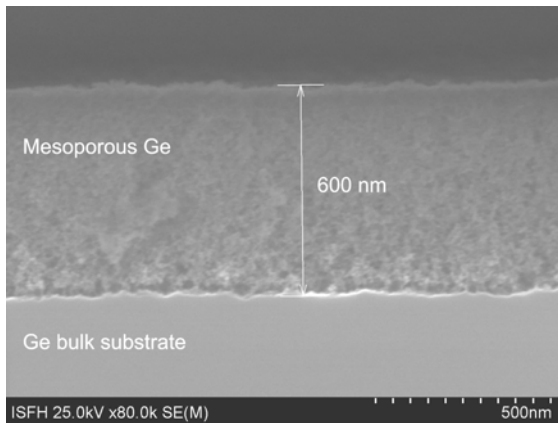


Figure 1: SEM image of the cross section of a PGe layer. (100) p-type Ge, HF 50 wt %, $j = 8.85 \text{ mA/cm}^2$, $t = 75 \text{ min}$.

Figure 2 shows a plane view of a electrochemically etched Ge substrate. Interference colours appear at the porous region, which are a result of Fabry-Perot interference fringes at the air/PGe and PGe/Ge substrate interfaces. The inner part of the wafer is homogeneously coloured, meaning that also the porosity and thickness of the porous layer is homogeneous. At the rim of the wafer, a stripe of different colour shows where the sample holder causes an inhomogeneous electrolyte flow and an increased electric field at the wafer edge. However, the SEM analysis shows a mean porous layer thickness of 200 nm with a maximal variation in the thickness of 30 nm within the inner (yellow/green) region.

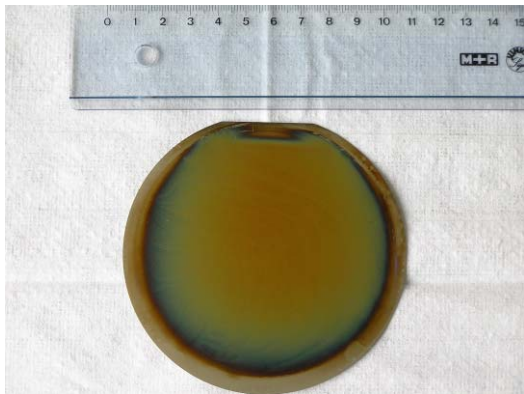


Figure 2: Ge wafer electrochemically etched. (100) p-type Ge, HF 40 wt %, $j = 5 \text{ mA/cm}^2$, $t = 3 \text{ h}$.

The lower part of the wafer is coloured blue more intensively than the upper part. Due to the higher density of HF compared to water, an increased concentration of HF at the bottom of the etching cell is observed after long etching durations of several hours. Mixing of the electrolyte during the etching process would enhance the homogeneity of the porous layer.

4 ETCHING RATES

Porous Ge formation by anodization takes place simultaneously with a constant dissolution of the already porosified surface. There are two etching fronts with different etching rates as the porous layer grows into the depth. On the one hand, the etching front at the bottom of the PGe layer is responsible of its growth. The porous

layer etching rate R_{etch} quantifies the velocity at which the porous layer grows into the sample. On the other hand, the already formed porous layer is continuously dissolved at its upper surface. The porous layer dissolution rate R_{diss} denotes the velocity at which the porous layer dissolves, limiting thus the growth rate of the porous layer. The difference between etching rate and dissolution rate gives the growth rate of the mesoporous layer R_{growth} . Figure 3 shows a schematic drawing of the different etching rates present during anodic etching.

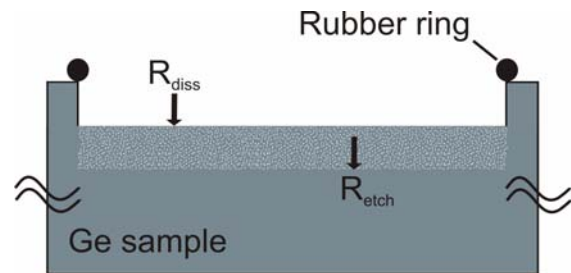


Figure 3: Porous Ge etching rates

R_{diss} is calculated by linearly fitting the remaining thickness of the substrate plus porous layer measured for different etching times at a given etching current density and electrolyte concentration. The slope of the linear fit gives the porous layer dissolution rate for each etching current density and electrolyte. Figure 4 shows the porous layer dissolution rates obtained for HF 40 wt % in water and ethanol, respectively, as a function of the etching current. We obtain dissolution rates in the range of 0.011 to 1.33 $\mu\text{m/minute}$ depending on the etching current applied and solvent used. We find two linear regimes in a semilogarithmic plot of the dissolution rates of the PGe layer shown in Figure 5, below and above 7.5 mA/cm^2 .

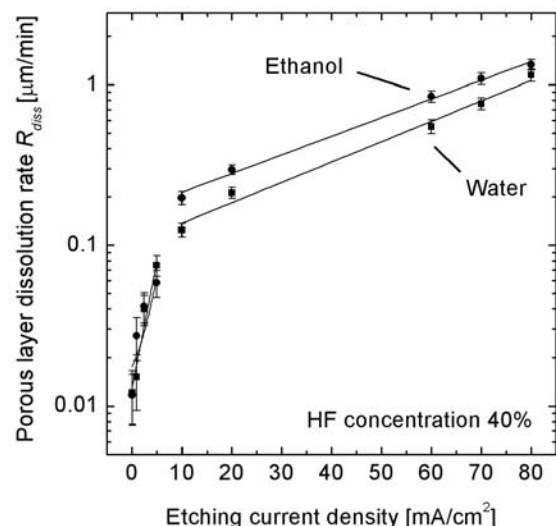


Figure 4: Porous layer dissolution rate vs. current applied.

A small variation in the low etching current density range implies a drastic change in the dissolution rate of the porous layer. However, a variation in the high current range affects the dissolution rate less. In order to avoid dissolution of the PGe layer, very low etching current densities have to be applied. Figure 4 shows that ethanoic electrolytes dissolve a larger amount of the substrate than

aqueous electrolytes. We relate this effect to the wetting properties of ethanol, as it enhances the wettability of the substrate and helps to remove hydrogen bubbles that are produced through the electrochemical etching of Ge. Since H_2 bubbles hinder PGe formation and etching, the use of ethanoic electrolytes allows a faster dissolution of the substrate.

We obtain R_{growth} from the slope of the linear fits of the measured porous layer thicknesses at different etching times for both aqueous and ethanoic electrolytes for each current density value. R_{growth} lies in the range between 0.071 and 2.7 nm/min for etching currents between 0.1 and 80 mA/cm². Figure 5 shows the porous layer growth rate as a function of the etching current density.

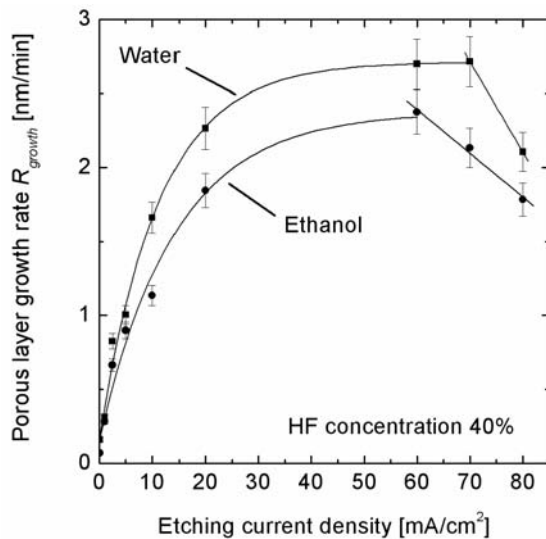


Figure 5: Porous layer growth rate vs. applied current.

Aqueous solutions show higher growth rates R_{growth} than ethanoic solutions. As mentioned before, this effect is related to the increased dissolution rate of the porous layer in ethanol. Since R_{growth} is given by the difference between the R_{etch} and R_{diss} , the porous layer etching rate is limited by R_{diss} . Ethanoic electrolytes present high dissolution rates R_{diss} , the fast dissolution of the porous layer therefore limits R_{growth} . High etching current densities above 60 mA/cm² lead to a linear decrease of R_{growth} for both ethanoic and aqueous electrolytes due to the increasing R_{diss} . Etching current densities higher than 80 mA/cm² do not even show porous layer formation as the increased R_{diss} simply leads to electropolishing of the wafer.

5 SUBSTRATE USAGE

We define the substrate usage $U=R_{growth}/R_{etch}$ as a parameter that quantifies the volume efficiency for transforming non-porous bulk material into porous material. Figure 6 shows the substrate usage of anodic porous Ge formation as a function of the etching current. Since R_{growth} is far smaller than R_{etch} , the usage is very low, in the range of 0.2 to 2.0%, showing thus very inefficient porous layer growth. Several μm of material are consumed in order to obtain a porous layer of a few hundreds of nanometers.

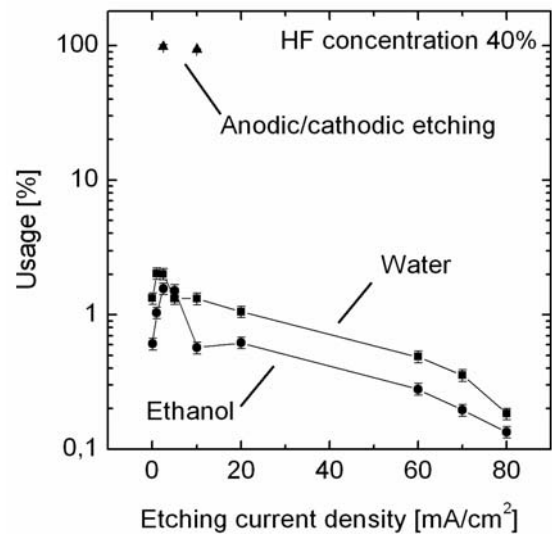


Figure 6: Usage vs. etching current density

Hydrogen passivation of the surface reduces substrate thinning. Turner carried out oscillographic investigations of the Ge surface by constantly changing the polarization direction [8]. He found the cathodic reactions to proceed in two steps: Firstly the Ge oxide at the surface is reduced. Secondly, hydrogen atoms bond to Ge surface atoms. The surface is thereby passivated, the porous layer stops to grow, and germane (soluble or gas) compounds form at the surface of the cathode. The reaction equation is



Choi and Buriak produced PGe by alternating the etching bias [9]. Fang et. al proposed a mechanism that increases the passivation of the Ge surface by switching the system periodically from anodic to cathodic bias [10]. The passivation provided by the cathodic step inhibits the dissolution of the already formed porous layer. However, the duration of the passivation is limited. It depends mainly on the etching current density of the subsequent anodic step and the electrolyte concentration. High etching current densities and electrolyte concentrations decrease the duration of passivation effect. Typically, passivation lasts 1 to 10 min. A new cathodic step is afterwards necessary in order to further passivate the surface. We pulse the system eight times from anodic to cathodic bias by changing the etching current density in order to passivate the surface.

Due to the increased passivation, R_{diss} decreases substantially, becoming almost zero. The passivation also affects R_{etch} , reducing the rate down to values similar to R_{growth} in the nm range. Since both, R_{growth} and R_{etch} , take similar values, the substrate usage increases substantially. Figure 7 shows that usage values in a range of 93 to 98% are obtained using this technique. The initial phase of porous layer growth, also called nucleation phase, causes substrate thinning until pore growth starts. This phase, common to all materials, usually removes a few microns of substrate until homogeneous nucleation is achieved. Higher usage values are therefore hardly possible due to initial substrate etching.

6 SUMMARY

We present the formation of mesoporous layers in Ge that are potentially suitable for lift-off processes and substrate reuse. The process is demonstrated on Ge wafers with 4" diameter, resulting in spatially homogenous porous layers. The formation of mesoporous Ge takes place simultaneously with a constant dissolution of the already formed porous layer. The dissolution rate of the already formed PGe lies in the range between 0.011 and 1.3 $\mu\text{m}/\text{min}$ for etching current density values between 0.1 and 80 mA/cm^2 respectively. The growth rate of the porous layer lies in a range between 0.071 and 2.71 nm/min . Thus, a considerable amount of the substrate wafer has to be etched off to obtain PGe layers of several hundreds of nm. In comparison to aqueous electrolytes, ethanoic solutions have a higher dissolution rate, which leads to more substrate thinning than with aqueous solutions. However, the porous layer growth rate is similar to the aqueous case. We presented a technique which allows porous Ge layer growth and avoids substrate thinning based on alternating between anodic to cathodic bias. The substrate usage drastically increases from values of 0.002 to 0.02 for anodically etched samples to values of 0.98 for samples using this technique. The etching rates and thicknesses achieved indicate that this technique may be compatible with lift-off processes for space solar cells.

7 ACKNOWLEDGMENTS

The authors would like to thank Sebastian Gatz, Andreas Wolf and Marco Ernst from the ISFH, Prof. Helmut Föll and Jürgen Carstensen from the University of Kiel, and Carsten Baur from European Space Agency for the fruitful discussions and Bianca Gehring for the technical assistance. The financial support of this work by the German Ministry for Economy and Technology under contract No. 50JR0641 is gratefully acknowledged. E. Garralaga Rojas specially thanks the European Space Agency for the financial support of his work in the framework of the Networking Partnering Initiative (Co. No. 20250/06/NL/GLC).

8 REFERENCES

- [1] M. Meusel, W. Bensch, T. Bergunde, R. Kern, V. Khorenko, W. Köstler, G. La Roche, T. Torunski, W. Zimmermann, G. Strobl, W. Guter, M. Hermle, R. Hoheisel, G. Siefer, E. Welser, F. Dimroth, A.W. Bett, W. Geens, C. Baur, S. Taylor, G. Hey, in *Proc. of the 22nd EUPVSEC*, Milano (2007), pp. 16-21.
- [2] M. Stan, D. Aiken, B. Clevenger, A. Cornfeld, J. Doman, E. Downard, J. Hills, R. Hoffman, G. Johnston, F. Newman, J. Pappan, A. Sandoval, P. Sharps, and J. Wood Jr., in *Proc. of the IEEE 4th WCPEC*, pp. 1865-1868 (2006).
- [3] Richard R. King, Christopher M. Fetzer, Daniel C. Law, Kenneth M. Edmondson, Hojun Yoon, Geoffrey S. Kinsey, Dimitri D. Krut, James H. Ermer, Peter Hebert, B. Terence Cavicchi, and Nasser H. Karam, in *Proc. of the IEEE 4th WCPEC*, pp. 1757-1762 (2006).
- [4] J. F. Geisz, S. Kurtz, M. W. Wanlass, J. S. Ward, A. Duda, D. J. Friedman, J. M. Olson, W. E. McMahon, T. E. Moriarty, and J. T. Kiehl, *Appl. Phys. Lett.* **91**, 023502 (2007).
- [5] R. Brendel, in *Proc. of the 14th EUPVSEC*, (WIP, Barcelona, 1997), pp. 1354-1357.
- [6] J. Rouquerol *et al.*, *Pure Appl. Chem.*, **66**, pp. 1739-1758, (1994).
- [7] E. Garralaga Rojas, H. Plagwitz, B. Terheiden, J. Hensen, C. Baur, G. La Roche, G.F.X. Strobl, and R. Brendel, *J. Electrochem. Soc.*, **156**, 8, pp. D310-D313 (2009).
- [8] D. Turner, *J. Electrochem. Soc.*, **103**, 252, (1956).
- [9] H.C. Choi and J. Buriak, *Chem. Comm.*, pp. 1669-1670, (2000).
- [10] C. Fang, H. Föll, and J. Carstensen, *J. Electroanal. Chem.*, **589**, pp. 259-288, (2006).